

Transcriptomic gene-network analysis of exposure to silver nanoparticle reveals potentially neurodegenerative progression in mouse brain neural cells

Ho-Chen Lin, Chin-Lin Huang, Yuh-Jeen Huang, I-Lun Hsiao, Chung-Wei Yang, Chun-Yu Chuang *

Department of Biomedical Engineering and Environmental Sciences, National Tsing Hua University, 101, Section 2, Kuang-Fu Road, Hsinchu 30013, Taiwan



ARTICLE INFO

Article history:

Received 12 January 2016

Received in revised form 30 March 2016

Accepted 24 April 2016

Available online 27 April 2016

Keywords:

Silver nanoparticle

Gene network

Beta amyloid

Neurodegenerative disease

Alzheimer's disease

ABSTRACT

Silver nanoparticles (AgNPs) are commonly used in daily living products. AgNPs can induce inflammatory response in neuronal cells, and potentially develop neurological disorders. The gene networks in response to AgNPs-induced neurodegenerative progression have not been clarified in various brain neural cells. This study found that 3–5 nm AgNPs were detectable to enter the nuclei of mouse neuronal cells after 24-h of exposure. The differentially expressed genes in mouse brain neural cells exposure to AgNPs were further identified using Phalanx Mouse OneArray® chip, and permitted to explore the gene network pathway regulating in neurodegenerative progression according to Cytoscape analysis. In focal adhesion pathway of ALT astrocytes, AgNPs induced the gene expression of RasGRF1 and reduced its downstream BCL2 gene for apoptosis. In cytosolic DNA sensing pathway of microglial BV2 cells, AgNPs reduced the gene expression of TREX1 and decreased IRF7 to release pro-inflammatory cytokines for inflammation and cellular activation. In MAPK pathway of neuronal N2a cells, AgNPs elevated GADD45 α gene expression, and attenuated its downstream PTPRR gene to interfere with neuron growth and differentiation. Moreover, AgNPs induced beta amyloid deposition in N2a cells, and decreased PSEN1 and PSEN2, which may disrupt calcium homeostasis and presynaptic dysfunction for Alzheimer's disease development. These findings suggested that AgNPs exposure reveals the potency to induce the progression of neurodegenerative disorder.

© 2016 Elsevier Ltd. All rights reserved.

1. Introduction

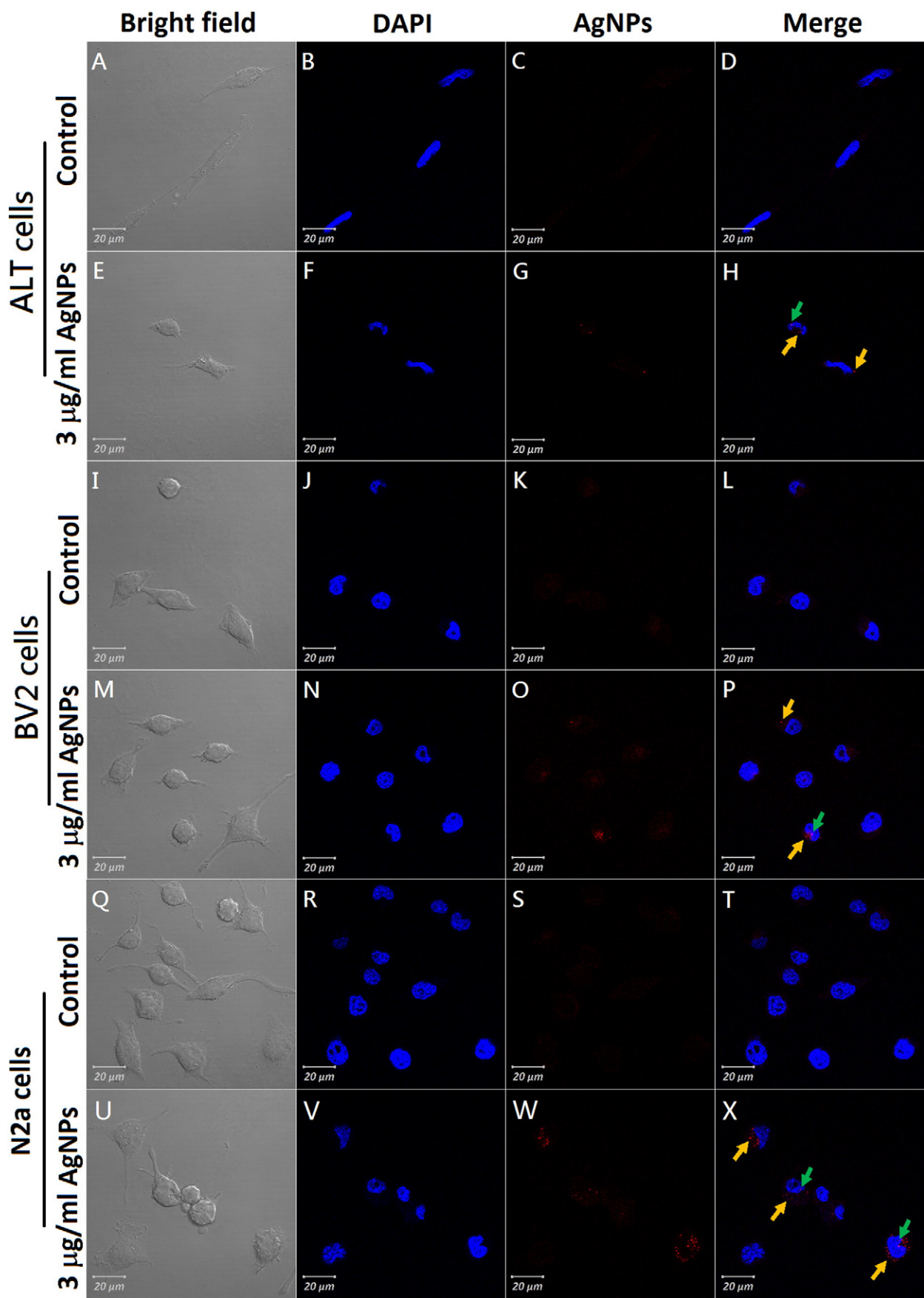
Silver nanoparticles (AgNPs) have antimicrobial characteristics commonly used in cosmetics, clothes, food containers, wound dressing and biomedical devices. The widespread AgNPs use increases AgNPs release to environment and enhances the risk of human exposure (Ribeiro et al., 2014). AgNPs are toxic to mammalian cells, e.g., liver, vascular system, lung, reproductive organs skin and brain (Ahamed et al., 2010). Both of AgNPs and Ag ion present cytotoxicity in vivo (Beer et al., 2012) and in vitro (Bilberg et al., 2012) studies, and lead to ultrastructural changes in synapses of the brain (Skalska et al., 2015). AgNPs (50–60 nm) can easily enter and accumulate in the mouse brain inducing neurotoxicity to alter cognitive functions and motor sensory (Sharma and Sharma, 2012). Moreover, AgNPs increase the protein expression of heme oxygenase 1 (HO-1) and enhance reactive oxygen species (ROS) generation to directly interfere with calcium responses and cause neuronal oxidative damage in primary mixed neural cells (Haase et al., 2012). Mice administered 25 nm of AgNPs produce neurotoxicity by generating free radical-induced oxidative stress and apoptosis in the frontal cortex, caudate and hippocampus (Rahman et al., 2009).

Alzheimer's disease (AD) is a progressive neurodegenerative disease presenting memory and learning dysfunction due to neuron death and synaptic degeneration (Arendt, 2009). The aggregated amyloid β (A β)40/A β 42 peptides are primary constituent of the plaques as the pathological hallmark in brain of AD patients (Ballard et al., 2011; Golde et al., 2000). Both A β 40 and A β 42 induce apoptotic cell death in cultured rat neuronal cells (Estus et al., 1997; Gschwind and Huber, 1995). The A β peptides generate from β -amyloid precursor protein (APP) were enzymatically cut by β - and γ -secretases (Wiltfang et al., 2007). Howlett and Richardson (2009) indicated that the accumulation of A β plaques was found in early age of APP transgenic mice.

Astrocytes, neuronal cells and microglial cells are main components of the brain. Astrocytes preserve neural environments buffering neurotransmitters and ions (Lian and Stringer, 2004). Microglia is the resident macrophage-like cell of the spinal cord and brain to release some cytokines and mediate neuroinflammatory processes (Wang et al., 2011). Neurons are specific cells to transmit information, and communicate with other nerve cells through chemical and electrical signals in the nervous system (Weiss et al., 2009). In the previous study, we have reported that 3–5 nm of AgNPs can enter mouse neuronal cells to induce pro-inflammatory cytokine production, and alter gene expressions related to A β deposition to induce AD progression (Huang et al., 2015). However, the potential gene network pathway of various brain neural cells in

* Corresponding author.

E-mail address: cychuang@mx.nthu.edu.tw (C.-Y. Chuang).



response to develop neurological disorders underlying AgNPs exposure has not been fully clarified. Thus, this study executed the gene network analysis to investigate whether 3–5 nm of AgNPs exposure altered gene expression corresponding to neurodegenerative progression in mouse brain astrocytes ALT cells, microglial BV2 cells, and neuron N2a cells.

2. Material and methods

2.1. Characteristic of AgNPs

The 12.625 $\mu\text{g/mL}$ of 3–5 nm uncoated AgNPs (Gold Nanotech, INC., Taiwan) which was stocked in deionized (DI) water were used in this study. According to JEM2100 transmission electron microscope (TEM; JEOL, Tokyo, Japan) image, the shapes of AgNPs were uniform in sphere, and the average size of them was 4.5 nm in DI water. The dynamic laser scattering (DLS) size of AgNPs was 114.5 ± 2.75 nm and 105.6 ± 20.26 nm respectively in DI water and in DMEM/10% FBS medium. The zeta potential of the AgNPs was 6.28 ± 0.338 mV and -5.5 ± 1.67 mV in DI water and in DMEM/10% FBS medium, individually. The concentration of silver ion in AgNPs stock solution was 0.17 $\mu\text{g/mL}$ according to perfectION™ comb Ag/S2 Combination Electrode (Mettler-Toledo Inc., Columbus, OH).

2.2. Cell culture and exposure

Three types of neural cells were used in this study. Mouse neuroblastoma neuro-2a (N2a) cells were cultured in high glucose Dulbecco's Modified Eagle's Medium (CORNING, New York) supplemented with 1% antibiotic (Biowest, Loire Valley, France), 1% sodium pyruvate (Invitrogen), 1% l-glutamine (Invitrogen) and 10% fetal bovine serum (Invitrogen, Carlsbad, Canada) in a cell incubator with 5% CO_2 at 37 °C. Murine microglial BV2 cells and murine brain ALT astrocytes were cultured in the similar medium with N2a cells except for the lack of 1% sodium pyruvate. Before AgNPs treatment, N2a cells were differentiated with 200 μM isobutylmethylxanthine (IBMX; SIGMA-Aldrich) and 30 μM forskolin (SIGMA-Aldrich, St. Louis, MO) for 48 h. The AgNPs were respectively added into the medium to treat ALT cells, BV2 cells and differentiated N2a cells for 24 h of exposure.

2.3. Confocal microscopy for AgNPs imaging in neural cells

Neural cells were individually cultured on glass coverslips with the treatment of AgNPs for 24 h. The cells were rinsed with the mixture solution of tripotassium hexacyanoferrate (III) (10 mM, SIGMA-Aldrich) and sodium thiosulfate pentahydrate (10 mM, SIGMA-Aldrich) to remove the AgNPs on cell surface. The cells were fixed in 4% paraformaldehyde (PFA) and covered by ProLong® antifade mountant with DAPI (Life Technologies, CA) for nuclei staining. Images were obtained by the confocal laser scanning microscopy (LSM 780, Carl Zeiss, Göttingen, Germany) with a $63 \times$ oil-immersion objective using 561 nm laser excitation for imaging AgNPs in reflectance mode and 405 nm laser for DAPI.

2.4. RNA extraction

Total RNA was extracted respectively from ALT cells, BV2 cells and differentiated N2a cells after 24 h of AgNPs exposure using RNA Trizol (Invitrogen). The quantity and purity of RNA samples were assessed using NanoDrop 2000c (Thermo, Wilmington, MA). The absorbance ratios of acceptable RNA purity are established at $A_{260}/A_{280} \geq 1.8$ and $A_{260}/A_{230} \geq 1.5$.

2.5. Reverse transcription and quantitative real-time PCR

cDNA was synthesized from 3 μg of total RNA by a high-capacity cDNA reverse transcription kit (Applied Biosystems, Foster City, CA). One hundred nanograms of cDNA was amplified by a real-time PCR with 40 cycles using 2 \times power SYBR green PCR master mix (Applied Biosystems). The primer sequences used were as follows: PSEN1 sense 5'-AGC AAC CGC CAG TGG AGA C-3' and anti-sense 5'-CGA AGT AGA ACA CGA GCC C-3'; PSEN2 sense 5'-GCC TGG GTC ATC TTG GGT G-3' and anti-sense 5'-TTT CTC TCC TGG GCA GTT TCC-3'; GADD45 α sense 5'-CAC TGT GTG CTG GTG ACG AAC-3' and anti-sense 5'-ACC CAC TGA TCC ATG TAG CGA C-3'; PTPRR sense 5'-ACC ATC CGC AAC CTC GTC-3' and anti-sense 5'-CTG GGC ACT GTC TGG AGT CTT AT-3'; TREX1 sense 5'-CAG CAT CTG TCA GTG GAA GCC-3' and anti-sense 5'-GCC AGG GGT GTA GTA GC-3'; IRF7 sense 5'-CCT TGG GTT CCT GGA TGT GA-3' and anti-sense 5'-AGA AGC GTC TCT GTG TAG TG-3'; RasGRF1 sense 5'-GGC CAC GTC GTG ACC CT-3' and anti-sense 5'-GCG TTT ACA GAT ACT TCC CTC G-3'; BCL2 sense 5'-TGT CAC AGA GGG GCT ACG AGT-3' and anti-sense 5'-TCA GGC TGG AAG GAG AAG ATG C-3'.

2.6. Transcriptomic profile determination

The gene expression profile of 9 μg total RNA of ALT cells, BV2 cells and differentiated N2a cells treated with AgNPs were individually determined using Mouse OneArray® v2.1 chips (Phalanx Biotech, Hsinchu, Taiwan). The intensities of fluorescent were extracted using GenePix 4.1 (Molecular Devices), and further normalized by Rosetta Resolver System (Rosetta Biosoftware, Seattle, WA).

2.7. Principal component analysis (PCA)

The genes of Phalanx microarray data (filtered by signal intensity >200) in neural cells exposure to AgNPs (0, 1, 2 and 3 $\mu\text{g/mL}$) were individually analyzed using the autoscaled method within ArrayTrack Software (U.S. Food and Drug Administration) to display the distribution of array data.

2.8. Gene ontology analysis

The differentially expressed genes (DEGs) were screened by $|\text{fold change}| \geq 1.2$ between two different treatments of AgNPs. Gene ontology (GO) analysis of DEGs was performed using DAVID website (<http://david.abcc.ncifcrf.gov/>).

2.9. Cytoscape analysis

The Cytoscape (Version 3.0.2) plug-in system "ClueGO + CluePedia" was used to identify networks and functional pathways of DEGs from AgNPs exposure chip data. Two-sided hypergeometric statistic was performed with kappa score threshold setting of 0.4, 0.4 and 0.3 in ALT cells, BV2 cells and N2a cells, respectively. A constructed gene network of AD was created in Cytoscape by importing the AD-related genes that resulted from integrating microarray datasets in a review paper (Bertram et al., 2010).

2.10. Western blotting for APP protein determination

N2a cells were lysed with RIPA buffer (Cell Signaling, Danvers, MA) containing proteinase inhibitor Cocktail (Sigma), and centrifuged at 14,000 g for 10 min at 4 °C. The supernatant were immediately

Fig. 1. AgNPs uptake in mouse neural cells. A confocal microscope was used to detect 3–5 nm of AgNPs distribution in ALT cells (A–H), BV2 cells (I–P) and N2a cells (Q–X). The cells were cultured in normal (A–D, I–L, Q–T) or containing 3 $\mu\text{g/mL}$ of AgNPs (E–H, M–P, U–X) culture medium for 24 h. The images of bright field (A, E, I, M, Q and U), DAPI staining (B, F, J, N, R and V) and AgNPs (C, G, K, O, S and W) were captured under confocal microscopy with $620 \times$ magnification. Yellow arrow: AgNPs located inside the cytoplasm; green arrows: AgNPs located in the nucleus; red color: AgNPs; blue color: nuclear marker DAPI. Scale bar = 20 μm .

Table 1GO analysis of the selected genes in ALT, BV2 and N2a cells treated with 2 and 3 μ g/mL of AgNPs.

ALT cells			BV2 cells			N2a cells		
GO term	Gene numbers	p-Value	GO term	Gene numbers	p-Value	GO term	Gene numbers	p-Value
Focal adhesion	201	1.42E-08	Cytosolic DNA-sensing pathway	56	6.80E-16	MAPK signalling pathway	267	3.60E-07
Glutathione conjugation	23	9.49E-07	Immune system process	41	2.70E-13	Regulation of biosynthetic Process	137	6.80E-06
IL6 pathway	47	6.53E-06	Response to virus	13	2.30E-10	Calcium signaling pathway	178	2.23E-06
B cell survival pathway	16	2.97E-06	Immune response	35	1.90E-09	Regulation of cellular metabolic process	154	2.15E-06
Cell adhesion	38	9.10E-04	Response to stimulus	68	1.27E-08	Endocytosis	183	7.99E-05
IL1 pathway	34	1.51E-04	Response to stress	39	3.50E-07	IFN- γ pathway	40	2.25E-05
Nervous system development	46	1.30E-02	Defense response	20	5.50E-06	Signaling by ILs	107	9.55E-04
Neuron projection development	16	1.70E-02	Innate immune response	10	1.00E-05	Intracellular signaling cascade	56	7.30E-04
Response to oxidative stress	10	6.10E-03	Positive regulation of cytokine production	5	8.40E-03	T cell receptor signaling pathway	108	1.81E-04
Cellular response to extracellular stimulus	8	1.30E-03	Regulation of immune system process	12	4.20E-03	Regulation of kinase activity	17	3.20E-03
Immune system process	40	6.60E-02	Phagocytosis	5	3.60E-03	Neurotransmitter release cycle	34	1.42E-03
Cell communication	30	5.10E-03	Immune effector process	8	1.60E-03	Regulation of MAP kinase activity	11	1.40E-03
Positive regulation of apoptosis	16	4.20E-02	Cell activation	8	4.90E-02	Cell differentiation	75	3.40E-02
Regulation of cell motion	12	2.20E-03	Aging	4	4.90E-02	Cell death	29	3.40E-02
Regulation of cell death	39	1.00E-03	Cell redox homeostasis	4	4.60E-02	Response to oxidative stress	8	4.90E-02

transferred, and the concentration was measured using a Bicinchoninic Acid Protein Assay Kit (Sigma). Protein in the samples were then electrophoresed over a 10% sodium dodecyl sulfate polyacrylamide gel, and subsequently transferred to a hydrophobic PVDF membrane (Millipore). The membrane-bound proteins were respectively immunostained with 1:1000 primary rabbit anti-mouse APP (Cat. EPR 5118-34, Abcam) or β -actin (Senta Cruz Biotechnology, Senta Cruz, CA) antibody and followed by treatment with secondary anti-rabbit IgG horseradish peroxidase (HRP) antibody (Senta Cruz Biotechnology, CA). The tagged proteins were detected using a chemiluminescence reagent (Thermo Scientific, Rockford, IL) and photographed in a G:Box ChemiXT 16 system (Syngene, Frederick, MD).

2.11. Immunofluorescent detection of $\text{A}\beta$ protein

Differentiated N2a cells were cultured on coverslips and fixed with 4% PFA. The cells were further permeabilized with 0.1% Triton X-100/PBS solution and blocked in 2% horse serum (HS). The coverslips incubated for 1 h with primary rabbit anti-mouse $\text{A}\beta$ 42 (1:500, Merck Millipore) and stained with secondary fluorescein isothiocyanate (FITC)-conjugated goat anti-rabbit IgG (1:500, Merck Millipore). Coverslips were mounted on slides in mounting medium. Immunofluorescence images were captured with an inverted microscope with fluorescence filters (Axio Observer A1/D1, Zeiss, Oberkochen, Germany).

2.12. Statistical analysis

The statistically significant differences of gene expression of real-time PCR among control and various doses of AgNPs treatment were analyzed using one-way ANOVA (SPSS package 13.0). All statistical significances were determined at two-tailed p-value <0.05 .

3. Results

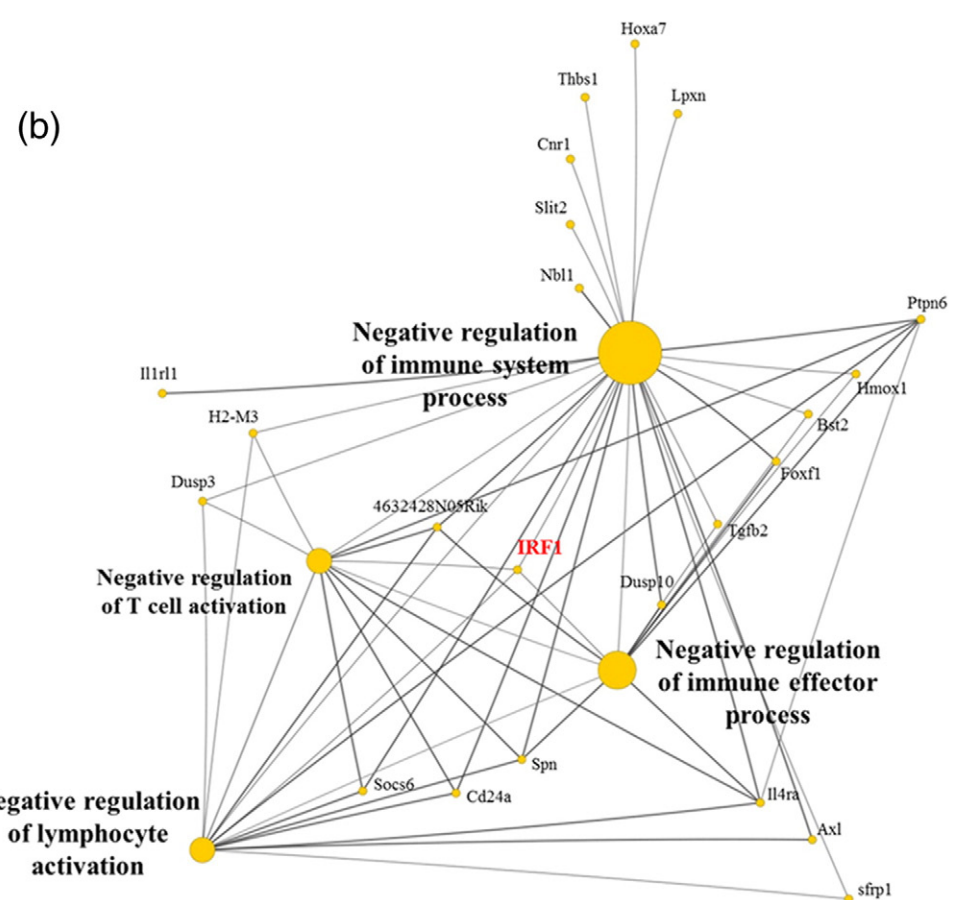
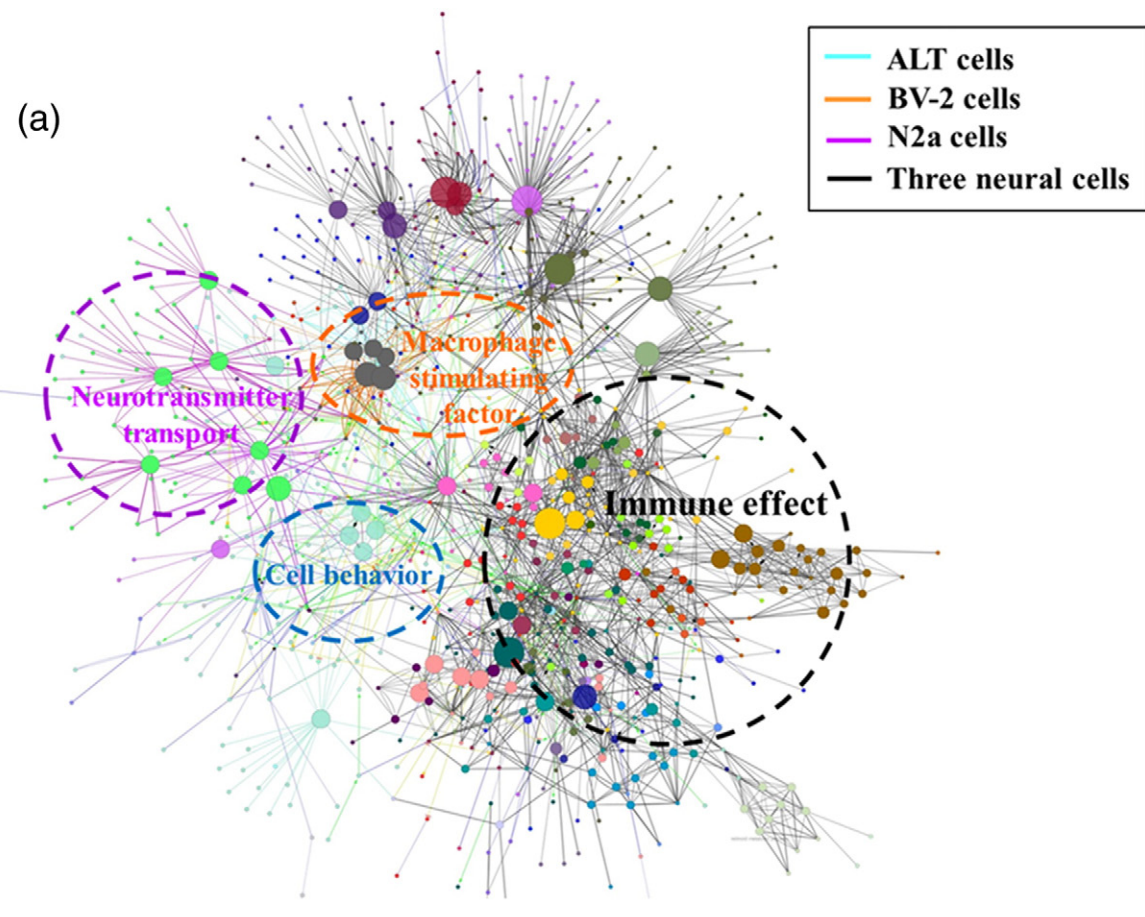
3.1. AgNPs can cross cell membrane and change gene expression in mouse neural cells

Under a confocal microscope, the 3–5 nm of AgNPs (3 μ g/mL) were observed to cross the cell membrane into the cytoplasm, and partially into the nucleus in three neural cells (Fig. 1). In analysis of Phalanx Mouse OneArray® chip, the PCA distribution presented the distinguishable dispersion among three various doses of AgNPs exposure in neural cells (Fig. S1). DEGs were selected according to the |fold change| of gene expression ≥ 1.2 between neural cells exposed to AgNPs and control. In ALT cells, the number of DEGs after 1, 2 and 3 μ g/mL of AgNPs exposure were respectively 585, 1295 and 2833 genes. In BV2 cells, there were 1013, 1008 and 533 DEGs individually in 1, 2 and 3 μ g/mL AgNPs exposure. The number of DEGs were 1789, 1278 and 2098 in N2a cells after 1, 2 and 3 μ g/mL of AgNPs exposure, respectively (Fig. S2). The 794, 291 and 801 DEGs were respectively in the intersections between ALT cells, BV2 cells and N2a cells exposed to 2 and 3 μ g/mL of AgNPs, and further used to analyze for GO and Cytoscape gene network. The fold change values of these DEGs expression were listed in Tables S1, S2 and S3.

3.2. Gene ontology of differentially expressed genes in neural cells exposure to AgNPs

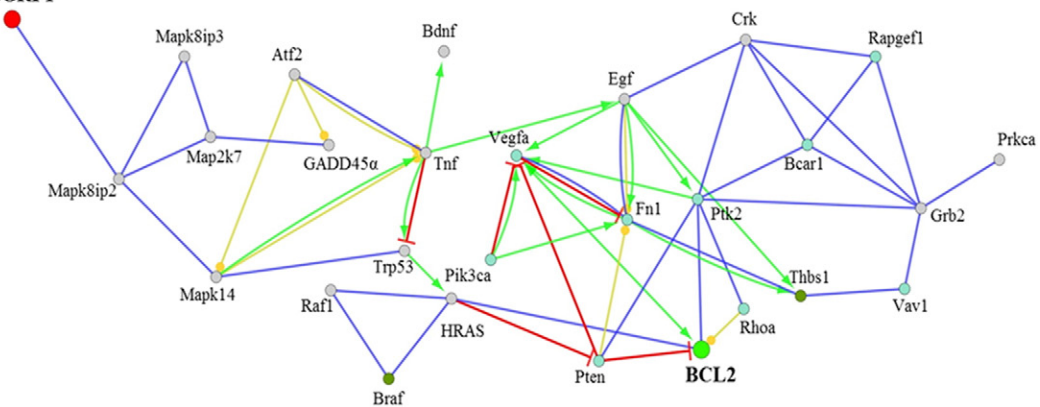
These intersections in the DEGs from neural cells exposed to AgNPs were examined in functional category analysis by GO website. In ALT cells, the 794 DEGs were relevant to focal adhesion, response to oxidative stress, regulation of immune response and cell behavior. In BV2 cells, the 291 DEGs were involved in cytosolic DNA-sensing pathway, response to stimulus, cell activation, immune response, defense response and inflammatory response. In N2a cells, the 801 DEGs were involved in MAPK signalling pathway, cell differentiation, regulation of

Fig. 2. A gene network in mouse neural cells exposure to AgNPs. (a) Totally 1886 DEGs of ALT cells, BV2 cells and N2a cells after AgNPs exposure (2 and 3 μ g/mL) were constructed a gene network. All of the three neural cells were involved in immune effect, and respectively regulated in the functions of cell behavior, macrophage stimulating factor, and neurotransmitter transport. (b) In immune effect function, the gene expression of IRF1 was regulated in ALT cells, BV2 cells and N2a cells after AgNPs exposure corresponding to immune system process, T cells activation, lymphocyte activation and immune effector process. In the interaction networks, each node represented as a cluster of genes, and the size and color of the nodes represented the fraction of the genes in the cluster sharing the same property.



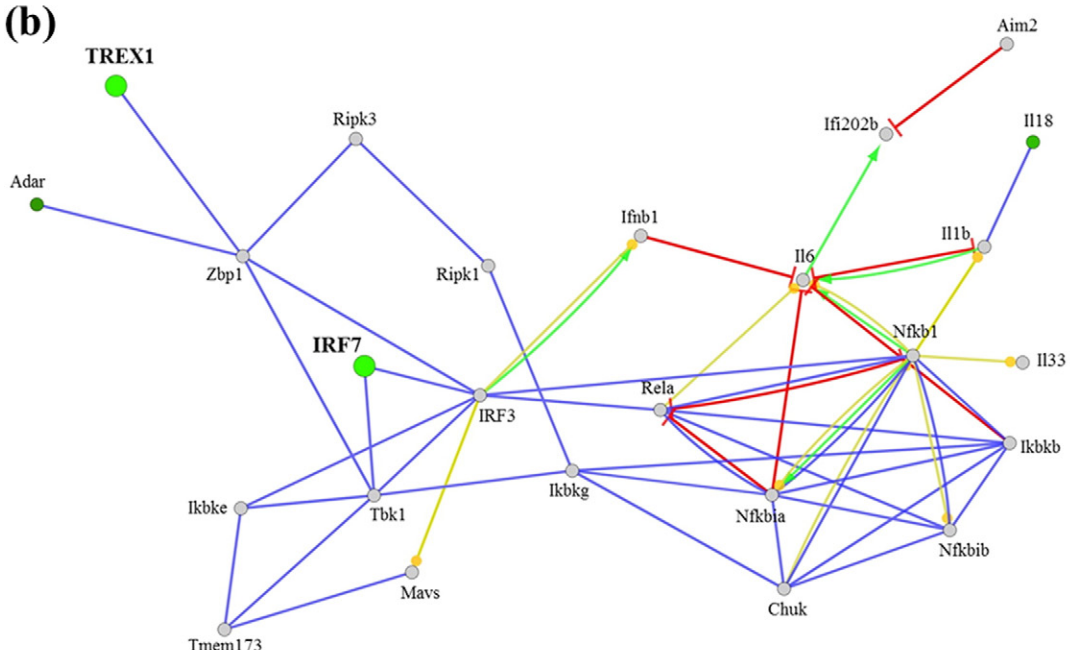
(a)

RasGRF1

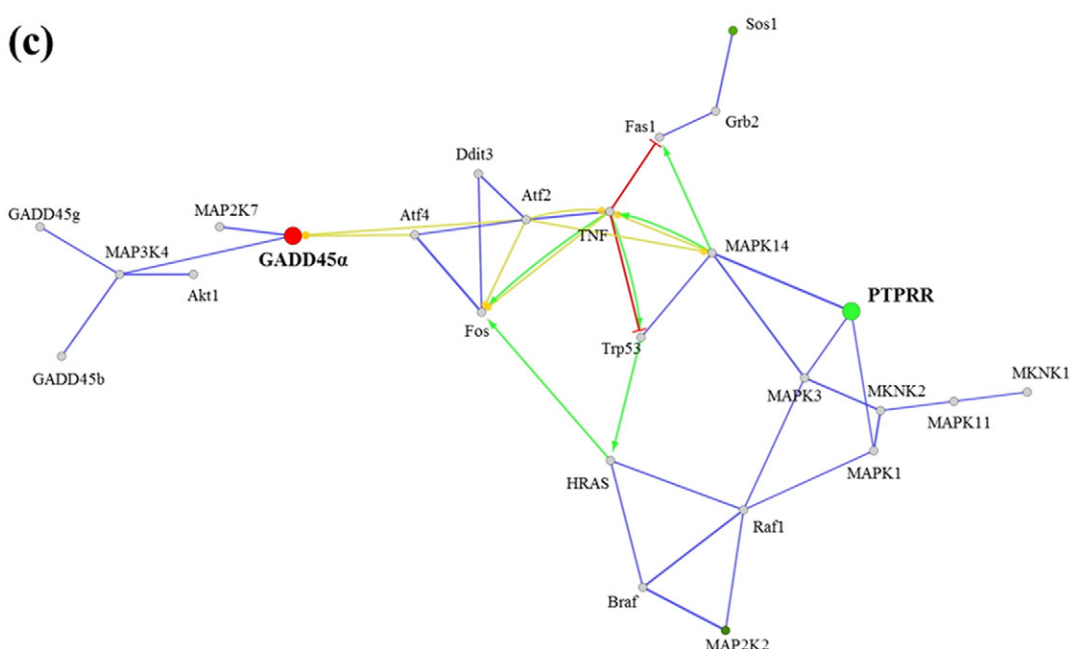


(b)

TREX1



(c)



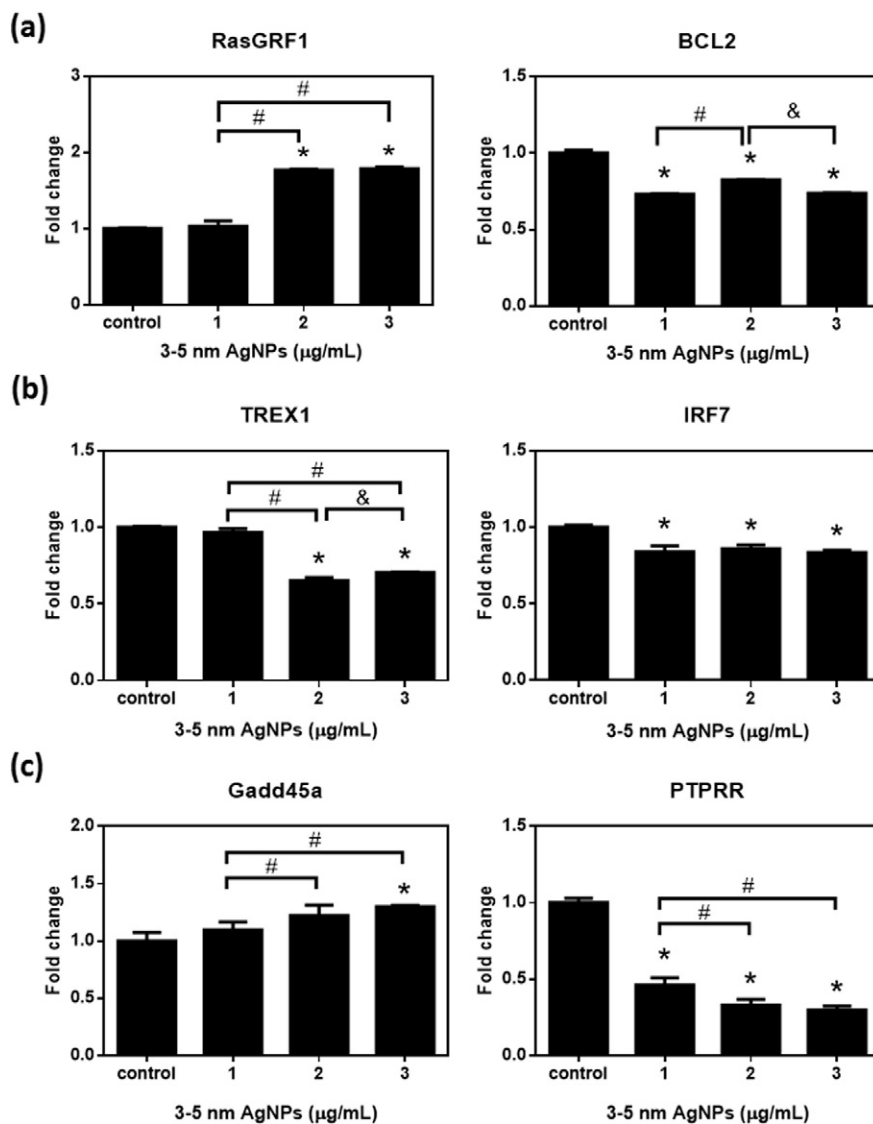


Fig. 4. Gene expression of three neural cells in exposure to AgNPs. The gene expressions were determined using a real-time PCR after 24 h of AgNP exposure (0, 1, 2 and 3 μ g/mL) in (a) ALT cells, (b) BV2 cells and (c) N2a cells. The data of three independent experiments were presented as mean \pm SD. *Indicated significant difference at $p < 0.05$ compared with control. #Indicated significant difference at $p < 0.05$ compared with 1 μ g/mL of AgNP exposure. &Indicated significant difference at $p < 0.05$ compared with 3 μ g/mL of AgNP exposure.

signal transduction, and cell communication (Table 1; Table S4 in detail).

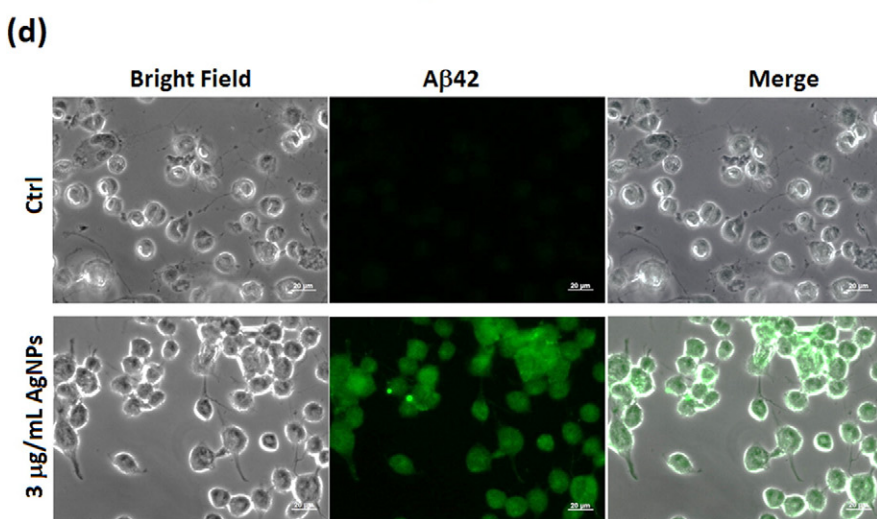
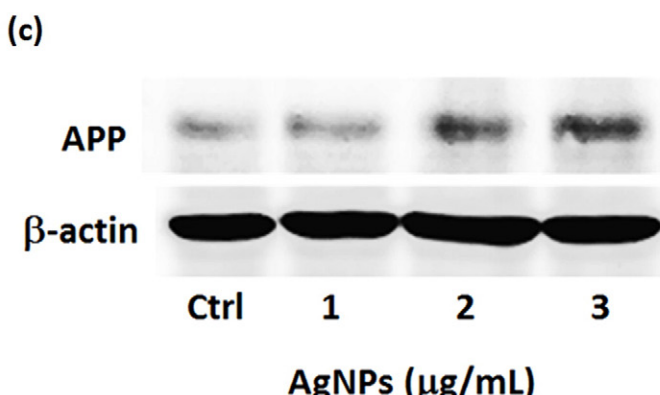
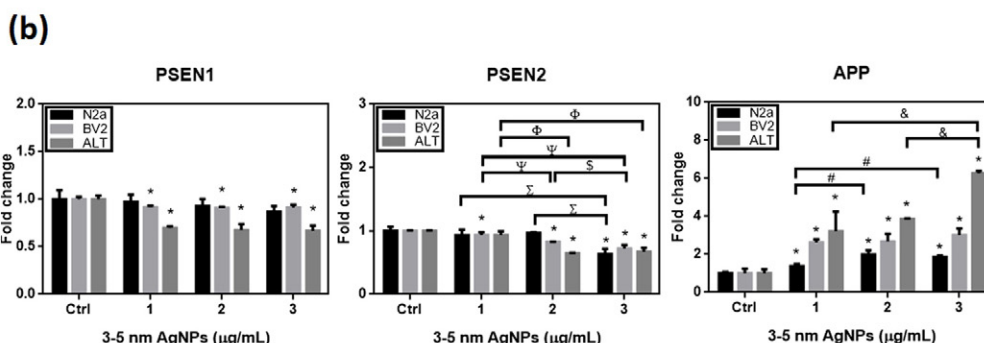
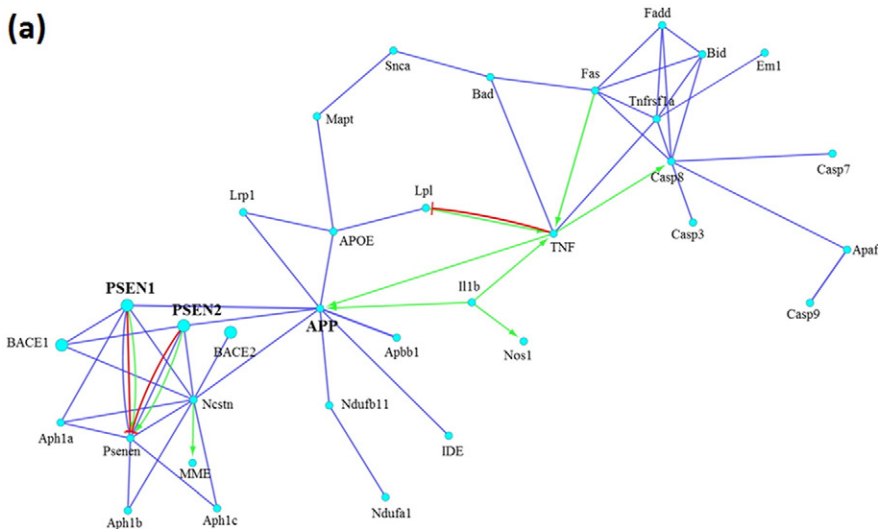
3.3. Gene network analysis in neural cells exposure to AgNPs

The total 1886 DEGs of three neural cells after 2 and 3 μ g/mL AgNPs exposure were subjected to gene network analysis by Cytoscape. Results showed that all of the three neural cells were in response to immune effect after AgNPs exposure. Moreover, ALT cells, BV2 cells, and N2a cells regulated the functions of cell behavior, macrophage stimulating factor, and neurotransmitter transport, respectively (Fig. 2a). The immune related genes were further analyzed, and the gene expression of interferon regulatory factor 1 (IRF1) was found to commonly alter in three neural cells after AgNPs exposure corresponding to the following immune system processes, T cells activation, lymphocyte activation and immune effector process (Fig. 2b).

3.4. Sub-networks of three neural cells in exposure to AgNPs

In ALT cells exposure to AgNPs, the GO functions of 794 DEGs in Cytoscape sub-network included cell adhesion, regulation of calcium-mediated signaling, ion transport and immune system process (Fig. S3). Focal adhesion pathway was selected according to GO analysis to represent in regulation of ALT cells after AgNPs exposure. In focal adhesion pathway of ALT cells (Fig. 3a), AgNPs exposure induced ras protein-specific guanine nucleotide-releasing factor 1 (RasGRF1) and decreased B-cell lymphoma 2 (BCL2) for sequestration of signaling molecules in survival signals to focal adhesions. RasGRF1 and BCL2 genes presented positively and negatively to regulate harvey rat sarcoma viral oncogene homolog (HRAS) gene, respectively. Results of real-time PCR showed that AgNPs significantly induced the gene expression of RasGRF1, and reduced BCL2 (Fig. 4a).

Fig. 3. Sub-network of neural cells in exposure to AgNPs. (a) In ALT cell exposure to AgNPs, focal adhesion pathway presented to induce RasGRF1 for activating HRAS and down-regulating BCL2. (b) In response to BV2 cells after AgNP exposure, cytosolic DNA-sensing pathway suppressed TREX1 and diminished IRF3/IRF7. (c) In N2a cells after AgNP exposure, MAPK pathway increased GADD45 α for activating TNF to decrease MAPK1 and subsequently down-regulate PTPRR genes. Green line: activation; blue line: binding; yellow line: expression; red line with a red bar: antagonizing.



In BV2 cells exposure to AgNPs, the GO functions of 291 DEGs in Cytoscape constructed sub-network included innate immune response, inflammatory response and interferon production (Fig. S4). Cytosolic DNA-sensing pathway was selected according to GO analysis to represent in regulation of BV2 cells after AgNPs exposure. In cytosolic DNA-sensing pathway of BV2 cells (Fig. 3b), AgNPs exposure decreased three-prime repair exonuclease 1 (TREX1) to diminish IRF3 and IRF7 for innate response and interferon (IFN) signaling in the pathogenesis of diseases. Results of real-time PCR showed that AgNPs significantly reduced the gene expression of TREX1 and IRF7 (Fig. 4b).

In N2a cells exposure to AgNPs, the GO functions of 801 DEGs in Cytoscape included regulation of mitogen-activated protein kinase (MAPK) activity, apoptotic process and neurotransmitter transport functions (Fig. S5). MAPK pathway can represent mostly in regulation of N2a cells after AgNPs exposure. In MAPK pathway of N2a cells (Fig. 3c), AgNPs exposure induced growth arrest and DNA-damage-inducible alpha (GADD45 α), and reduced protein tyrosine phosphatase receptor-type R (PTPRR) for sequestration of signaling molecules to maintain genomic stability, apoptosis and regulate the ion channels and receptors. Results of real-time PCR showed that AgNPs significantly increased the gene expression of GADD45 α and reduced PTPRR (Fig. 4c).

3.5. Determination of AgNPs-induced DEGs and A β in AD pathway

The constructed gene network of AD pathway presented that presenilin-1 (PSEN1) and PSEN2 genes interacted with APP gene to alter APP protein metabolism (Fig. 5a). Results of real-time PCR showed that AgNPs exposure substantially decreased the gene expression of PSEN1 in ALT cells and BV2 cells, and decreased PSEN2 while increasing APP in all of the three neural cells (Fig. 5b). The result of Western blot showed that APP protein was induced to express in N2a cells after 2 and 3 μ g/mL of AgNPs treatment for 24 h (Fig. 5c). The immunofluorescent images revealed that AgNPs exposure enhance A β 42 protein production in N2a cells (Fig. 5d).

4. Discussion

This study found that 3–5 nm of AgNPs can enter neural cells in the cytoplasm and nucleus (Fig. 1). According to the serial gene network analysis, AgNPs exposure altered the gene expression of neural cells corresponding to immune response (Fig. 2), focal adhesion pathway (Fig. 3a), cytosolic DNA sensing pathway (Fig. 3b) and MAPK pathway (Fig. 3c), which might release inflammatory cytokines and cause DNA damage to induce cell apoptosis. Furthermore, AgNPs exposure decreased PSEN1 and PSEN2, and induced APP gene and its protein expression (Fig. 5b and c). It also deposited A β 42 protein (Fig. 5d) in neuronal cells potentially to disrupt calcium homeostasis and presynaptic dysfunction for the progression of neurodegenerative disorders.

4.1. AgNPs changed the gene expressions of immune pathway in neural cells

This study found that AgNPs can pass through the cell membrane into the nucleus of neural cells to further alter gene expression. The Cytoscape gene network analysis in this study found that IRF1 was

commonly regulated in mouse neural ALT cells, BV2 cells and N2a cells after AgNPs exposure (Fig. 2b). IRF1 is a critical gene in immune response, apoptosis and DNA damage, which stimulates cytokines and cyclin-dependent kinase inhibitor 1A (CDKN1A) gene expression (Kirchhoff et al., 2000). IRF1 participates in IFN- γ signaling pathway to regulate the genes of innate and adaptive immunity (Shi et al., 2011) and mediates immune surveillance in response to inflammatory reaction (Ksienzyk et al., 2012; Ksienzyk et al., 2011).

4.2. AgNPs changed the gene expressions in ALT cells, BV2 cells and N2a cells

In ALT cells exposure to AgNPs, the gene expression of RasGRF1 and BCL2 in focal adhesion pathway was up-regulated (Fig. 4a). Ratajczak et al. (2011) indicated that RasGRF1-deficient mice increase the lifespan. Calcium ions regulate RasGRF1 (Gudermann and Roelle, 2006) to activate HRAS expression (Arozarena et al., 2004), and down-regulate the downstream BCL2 gene (Nakayamada et al., 2003). Ola et al. (2011) pointed that BCL2 is a negative regulator able to modulate cell death through regulating mitochondria to release apoptotic mediators. The BCL2-deficient mice generate a variety of abnormality symptom including excessive cell death. Mice lacking BCL2 reduce glutathione peroxidase activity and glutathione levels in brain tissue (Hochman et al., 1998), and increase the susceptibility of mitochondrial oxidative stress to cause neuronal cell death (Wilkins et al., 2012).

In BV2 cells exposure to AgNPs, TREX1 and IRF7 expressions relevant to cytosolic DNA-sensing pathway were significantly decreased (Fig. 4b). Pereira-Lopes et al. (2013) pointed that the absence of TREX1 in mice enhances the production of proinflammatory cytokines tumor necrosis factor alpha (TNF- α), IFN type 1 and IL-1 β , and have inflammatory signatures in various organs including brain. TREX1-deficient mice have the eliminated transcription factor IRF3 expression (Vilaysane and Muruve, 2009). A study indicated that IRF7 interacts with IRF3 to regulate inflammatory response (Hasan et al., 2013). The IRF7-deficient mice increase the gene expression of cytokine and chemokine such as C-X-C motif chemokine 10 (CXCL10), C-C motif ligand 2 (CCL2), IL-17 and IL-1 β to affect inflammatory response (Salem et al., 2011).

In N2a cells, AgNPs exposure enhanced GADD45 α and decreased PTPRR mRNA levels in MAPK pathway (Fig. 4c). Overexpression of GADD45 α gene significantly impairs the morphology of neurons and reduces the neurite complexity in *in vitro* and *in vivo* experiments (Sarkisian and Siebzehnrubl, 2012). The up-regulated GADD45 α gene expression activates TNF (Tryndyak et al., 2010) to decrease MAPK1 (Eliopoulos et al., 2003) and PTPRR (Hendriks et al., 2009). PTPRR plays a critical role in cerebellum motor function in neural tissue. The absence of PTPRR in mice is observed to defect in their subtle motor coordination and balance skills (Chirivi et al., 2007).

The above results suggested that AgNPs exposure might induce the gene expression of RasGRF1 and reduce BCL2 in ALT astrocytes to cause cell apoptosis, and reduce the gene expression of TREX1 and IRF7 to release pro-inflammatory cytokines for inflammation and cellular activation in microglial BV2 cells. Furthermore, AgNPs could induce GADD45 α and reduce PTPRR gene in neuronal N2a cells to interfere with neuron growth and differentiation, cerebellum motor coordination, and balance skills.

Fig. 5. AgNPs exposure changed gene expression relevant to the gene network of Alzheimer's disease progression, and increased beta amyloid deposition in N2a cells. (a) A constructed gene network of Alzheimer's disease presented that PSEN1 and PSEN2 genes interacted with APP gene to alter APP protein metabolism. Green line: activation; blue line: binding; yellow line: expression; red line with a red bar: antagonizing. (b) Gene expressions of PSEN1, PSEN2 and APP in N2a cells after AgNPs exposure. The gene expressions were determined using a real-time PCR after 24 h of AgNPs exposure (0, 1, 2 and 3 μ g/mL). The data of three independent experiments were presented as mean \pm SD. *Indicated significant difference at $p < 0.05$ compared with control. #Indicated significant difference at $p < 0.05$ compared with 1 μ g/mL of AgNPs exposure. ‡ Indicated significant difference at $p < 0.05$ compared with 3 μ g/mL of AgNPs exposure. (c) Western blot determination of APP protein in N2a cells after AgNPs exposure. The 40 μ g of total proteins were loaded for Western blot to determine APP protein in N2a cells exposure to 1, 2 and 3 μ g/mL of AgNPs for 24 h. (d) A β 42 plaque generation in N2a cells after AgNPs exposure. Immunofluorescent detection of primary rabbit anti-mouse A β 42 was stained with secondary goat FITC-conjugated anti-rabbit IgG in N2a cells after 24 h 3 μ g/mL 3–5 nm of AgNPs treatment. The control groups and AgNPs exposure groups were taken under 200 \times magnification at 150 ms and 500 ms exposure time respectively for bright field and primary rabbit anti-mouse A β 42.

4.3. Potential mechanism of AD pathogenesis in mouse neural cells exposure to AgNPs

The present study showed AgNPs exposure down-regulated PSEN1 and PSEN2 gene expression in the pathogenesis of Alzheimer's disease (Fig. 5b). PSEN1 in brain performs in cellular signaling. Loss of PSEN1 leads to abnormalities in glia-guided radial migration and tangential migration in mice cerebellar morphogenesis (Louvi et al., 2004). PSEN2 dysfunction influences CNS development and evokes inflammatory response. Lack of PSEN2 function expands the pro-inflammatory responses in primary microglia of brain cortices in perinatal mice (Jayadev et al., 2013). PSEN1 and PSEN2 regulate calcium homeostasis and synaptic function via ryanodine receptor. Loss of PSEN1 and PSEN2 function impairs calcium ion release and reduces neurotransmitter release (e.g., glutamate) to lead to the impairment of presynaptic terminals (Pimplikar et al., 2010). The disrupted intracellular calcium homeostasis can cause presynaptic dysfunction and develop AD pathogenesis (Wu et al., 2013). Delabio et al. (2014) indicated PSEN2 in AD patients were significantly decreased in the auditory cortex.

Moreover, this study found that AgNPs induced APP gene and enhanced A β 42 deposition in neuronal cells. Bateman et al. (2006) indicated that a large quantity of APP is continuously metabolized to A β in the brain. The increased concentration of A β 42 in the brain promotes the development of early Alzheimer's disease (Steinerman et al., 2008). Amyloid-dependent pathway and amyloid-independent pathway (Pimplikar et al., 2010) are two mechanisms of AD pathogenesis. The amyloid-dependent pathway causes A β deposition, which leads to AD; furthermore, amyloid-independent pathway influences the signal transmission and causes synaptic dysfunction to evolve AD pathogenesis (Hyman, 2011). After AgNPs exposure, the decreased expression of PSEN1 and PSEN2 in neuronal cells was observed in this study. It suggested that AgNPs exposure might cause AD pathogenesis via both amyloid-dependent and amyloid-independent pathway.

5. Conclusion

In summary, this study found that 3–5 nm of AgNPs enter the nucleus of mouse neural cells, and alter gene networks corresponding to focal adhesion pathway, cytosolic DNA-sensing pathway, MAPK pathway, and immune response potentially enhancing apoptosis in neuronal cells. Furthermore, AgNPs decreased gene expressions of PSEN1 and PSEN2, and induced APP to A β deposition potentially contributing to the development of neuron function disorder. These findings suggested that AgNPs exposure might evolve neurodegenerative disease progression relevant to Alzheimer's disease.

Supplementary data to this article can be found online at <http://dx.doi.org/10.1016/j.tiv.2016.04.014>.

Funding sources

This study was supported by Taiwan Ministry of Science and Technology grant 103-2221-E-007-006-MY3.

Transparency document

The transparency document associated with this article can be found, in online version.

Acknowledgment

We thank Gold Nanotech, Inc., Taiwan for providing AgNPs material in this collaborative research, and the excellent detection technique of confocal laser microscopy in Technology Commons, College of Biomedical Science and Engineering Center, National Tsing Hua University, Taiwan.

References

Ahamed, M., Alsahli, M.S., Siddiqui, M.K., 2010. Silver nanoparticle applications and human health. *Clin. Chim. Acta* 411, 1841–1848. <http://dx.doi.org/10.1016/j.cca.2010.08.016>.

Arendt, T., 2009. Synaptic degeneration in Alzheimer's disease. *Acta Neuropathol.* 118, 167–179. <http://dx.doi.org/10.1007/s00401-009-0536-x>.

Arozarena, I., Matañanas, D., Berciano, M.T., Sanz-Moreno, V., Calvo, F., Munoz, M.T., Egea, G., Lafarga, M., Crespo, P., 2004. Activation of H-Ras in the endoplasmic reticulum by the RasGRF family guanine nucleotide exchange factors. *Mol. Cell. Biol.* 24, 1516–1530. <http://dx.doi.org/10.1128/MCB.24.4.1516-1530.2004>.

Ballard, C., Gauthier, S., Corbett, A., Brayne, C., Aarsland, D., Jones, E., 2011. Alzheimer's disease. *Lancet* 377, 1019–1031. [http://dx.doi.org/10.1016/S0140-6736\(10\)61349-9](http://dx.doi.org/10.1016/S0140-6736(10)61349-9).

Bateman, R.J., Munsell, L.Y., Morris, J.C., Swarm, R., Yarasheski, K.E., Holtzman, D.M., 2006. Human amyloid-beta synthesis and clearance rates as measured in cerebrospinal fluid in vivo. *Nat. Med.* 12, 856–861. <http://dx.doi.org/10.1038/nm1438>.

Beer, C., Foldbjerg, R., Hayashi, Y., Sutherland, D.S., Autrup, H., 2012. Toxicity of silver nanoparticles – nanoparticle or silver ion? *Toxicol. Lett.* 208, 286–292. <http://dx.doi.org/10.1016/j.toxlet.2011.11.002>.

Bertram, L., Lill, C.M., Tanzi, R.E., 2010. The genetics of Alzheimer disease: back to the future. *Neuron* 68, 270–281. <http://dx.doi.org/10.1016/j.neuron.2010.10.013>.

Bilberg, K., Hovgaard, M.B., Besenbacher, F., Baattrup, E., 2012. In vivo toxicity of silver nanoparticles and silver ions in zebrafish (*Danio rerio*). *J. Toxicol.* 2012, 293784. <http://dx.doi.org/10.1155/2012/293784>.

Chirivi, R.G., Noordman, Y.E., Van der Zee, C.E., Hendriks, W.J., 2007. Altered MAP kinase phosphorylation and impaired motor coordination in PTPRR deficient mice. *J. Neurochem.* 101, 829–840. <http://dx.doi.org/10.1111/j.1471-4159.2006.04398.x>.

Delabio, R., Rasmussen, L., Mizumoto, I., Viani, G.A., Chen, E., Villares, J., Costa, I.B., Turecki, G., Linde, S.A., Smith, M.C., Payao, S.L., 2014. PSEN1 and PSEN2 gene expression in Alzheimer's disease brain: a new approach. *J. Alzheimers Dis.* 42, 757–760. <http://dx.doi.org/10.3233/JAD-140033>.

Eliopoulos, A.G., Wang, C.C., Dumitru, C.D., Tsichlis, P.N., 2003. Tpl2 transduces CD40 and TNF signals that activate ERK and regulates IgE induction by CD40. *EMBO J.* 22, 3855–3864. <http://dx.doi.org/10.1093/emboj/cdg386>.

Estus, S., Tucker, H.M., van Rooyen, C., Wright, S., Brigham, E.F., Wogulis, M., Rydel, R.E., 1997. Aggregated amyloid-beta protein induces cortical neuronal apoptosis and concomitant "apoptotic" pattern of gene induction. *J. Neurosci.* 17, 7736–7745.

Golde, T.E., Eckman, C.B., Younkin, S.G., 2000. Biochemical detection of Abeta isoforms: implications for pathogenesis, diagnosis, and treatment of Alzheimer's disease. *Biochim. Biophys. Acta* 1502, 172–187. [http://dx.doi.org/10.1016/S0925-4439\(00\)00043-0](http://dx.doi.org/10.1016/S0925-4439(00)00043-0).

Gschwind, M., Huber, G., 1995. Apoptotic cell death induced by beta-amyloid 1–42 peptide is cell type dependent. *J. Neurochem.* 65, 292–300. <http://dx.doi.org/10.1046/j.1471-4159.1995.65010292.x>.

Gudermann, T., Roelle, S., 2006. Calcium-dependent growth regulation of small cell lung cancer cells by neuropeptides. *Endocr. Relat. Cancer* 13, 1069–1084. <http://dx.doi.org/10.1677/erc.1.01302>.

Haase, A., Rott, S., Mantion, A., Graf, P., Plendl, J., Thunemann, A.F., Meier, W.P., Taubert, A., Luch, A., Reiser, G., 2012. Effects of silver nanoparticles on primary mixed neural cell cultures: uptake, oxidative stress and acute calcium responses. *Toxicol. Sci.* 126, 457–468. <http://dx.doi.org/10.1093/toxsci/kfs003>.

Hasan, M., Koch, J., Rakheja, D., Pattnaik, A.K., Brugarolas, J., Dozmanov, I., Levine, B., Wakeland, E.K., Lee-Kirsch, M.A., Yan, N., 2013. Trex1 regulates lysosomal biogenesis and interferon-independent activation of antiviral genes. *Nat. Immunol.* 14, 61–71. <http://dx.doi.org/10.1038/ni.2475>.

Hendriks, W.J., Dilaver, G., Noordman, Y.E., Kremer, B., Fransen, J.A., 2009. PTPRR protein tyrosine phosphatase isoforms and locomotion of vesicles and mice. *Cerebellum* 8, 80–88. <http://dx.doi.org/10.1007/s12311-008-0088-y>.

Hochman, A., Sternin, H., Gorodin, S., Korsmeyer, S., Ziv, I., Melamed, E., Offen, D., 1998. Enhanced oxidative stress and altered antioxidants in brains of Bcl-2-deficient mice. *J. Neurochem.* 71, 741–748. <http://dx.doi.org/10.1046/j.1471-4159.1998.71020741.x>.

Howlett, D.R., Richardson, J.C., 2009. The pathology of APP transgenic mice: a model of Alzheimer's disease or simply overexpression of APP? *Histol. Histopathol.* 24, 83–100.

Huang, C.L., Hsiao, I.L., Lin, H.C., Wang, C.F., Huang, Y.J., Chuang, C.Y., 2015. Silver nanoparticles affect on gene expression of inflammatory and neurodegenerative responses in mouse brain neural cells. *Environ. Res.* 136, 253–263. <http://dx.doi.org/10.1016/j.envres.2014.11.006>.

Hyman, B.T., 2011. Amyloid-dependent and amyloid-independent stages of Alzheimer disease. *Arch. Neurol.* 68, 1062–1064. <http://dx.doi.org/10.1001/archneurol.2011.70>.

Jayadev, S., Case, A., Alajajian, B., Eastman, A.J., Moller, T., Garden, G.A., 2013. Presenilin 2 influences miR146 level and activity in microglia. *J. Neurochem.* 127, 592–599. <http://dx.doi.org/10.1111/jnc.12400>.

Kirchhoff, S., Oumard, A., Nourbakhsh, M., Levi, B.Z., Hauser, H., 2000. Interplay between repressing and activating domains defines the transcriptional activity of IRF-1. *Eur. J. Biochem.* 267, 6753–6761. <http://dx.doi.org/10.1046/j.1432-1327.2000.01750.x>.

Ksienzyk, A., Neumann, B., Nandakumar, R., Finsterbusch, K., Grashoff, M., Zawatzky, R., Bernhardt, G., Hauser, H., Kroger, A., 2011. IRF-1 expression is essential for natural killer cells to suppress metastasis. *Cancer Res.* 71, 6410–6418. <http://dx.doi.org/10.1158/0008-5472.CAN-11-1565>.

Ksienzyk, A., Neumann, B., Kroger, A., 2012. IRF-1 is critical for IFNgamma mediated immune surveillance. *Oncoimmunology* 1, 533–534. <http://dx.doi.org/10.4161/onci.19405>.

Lian, X.Y., Stringer, J.L., 2004. Astrocytes contribute to regulation of extracellular calcium and potassium in the rat cerebral cortex during spreading depression. *Brain Res.* 1012, 177–184. <http://dx.doi.org/10.1016/j.brainres.2004.04.011>.

Louvi, A., Sisodia, S.S., Grove, E.A., 2004. Presenilin 1 in migration and morphogenesis in the central nervous system. *Development* 131, 3093–3105. <http://dx.doi.org/10.1242/dev.01191>.

Nakayamada, S., Okada, Y., Saito, K., Tamura, M., Tanaka, Y., 2003. Beta1 integrin/focal adhesion kinase-mediated signalling induces intercellular adhesion molecule 1 and receptor activator of nuclear factor kappaB ligand on osteoblasts and osteoclast maturation. *J. Biol. Chem.* 278, 45368–45374. <http://dx.doi.org/10.1074/jbc.M308786200>.

Ola, M.S., Nawaz, M., Ahsan, H., 2011. Role of Bcl-2 family proteins and caspases in the regulation of apoptosis. *Mol. Cell. Biochem.* 351, 41–58. <http://dx.doi.org/10.1007/s11010-010-0709-x>.

Pereira-Lopes, S., Celhar, T., Sans-Fons, G., Serra, M., Fairhurst, A.M., Lloberas, J., Celada, A., 2013. The exonuclease Trex1 restrains macrophage proinflammatory activation. *J. Immunol.* 191, 6128–6135. <http://dx.doi.org/10.4049/jimmunol.1301603>.

Pimplikar, S.W., Nixon, R.A., Robakis, N.K., Shen, J., Tsai, L.H., 2010. Amyloid-independent mechanisms in Alzheimer's disease pathogenesis. *J. Neurosci.* 30, 14946–14954. <http://dx.doi.org/10.1523/JNEUROSCI.4305-10.2010>.

Rahman, M.F., Wang, J., Patterson, T.A., Saini, U.T., Robinson, B.L., Newport, G.D., Murdock, R.C., Schlagel, J.J., Hussain, S.M., Ali, S.F., 2009. Expression of genes related to oxidative stress in the mouse brain after exposure to silver-25 nanoparticles. *Toxicol. Lett.* 187, 15–21. <http://dx.doi.org/10.1016/j.toxlet.2009.01.020>.

Ratajczak, M.Z., Kucia, M., Liu, R., Shin, D.M., Bryndza, E., Masternak, M.M., Tarnowski, M., Ratajczak, J., Bartke, A., 2011. *RasGrf1: genomic imprinting, VSELs, and aging*. *Aging (Albany NY)* 3, 692–697.

Ribeiro, F., Gallego-Urrea, J.A., Jurkschat, K., Crossley, A., Hasselvold, M., Taylor, C., Soares, A.M., Loureiro, S., 2014. Silver nanoparticles and silver nitrate induce high toxicity to *Pseudokirchneriella subcapitata*, *Daphnia magna* and *Danio rerio*. *Sci. Total Environ.* 466–467, 232–241. <http://dx.doi.org/10.1016/j.scitotenv.2013.06.101>.

Salem, M., Mony, J.T., Lobner, M., Khoroshi, R., Owens, T., 2011. Interferon regulatory factor-7 modulates experimental autoimmune encephalomyelitis in mice. *J. Neuroinflammation* 8, 181. <http://dx.doi.org/10.1186/1742-2094-8-181>.

Sarkisian, M.R., Siebzehnruhl, D., 2012. Abnormal levels of Gadd45alpha in developing neocortex impair neurite outgrowth. *PLoS One* 7, e44207. <http://dx.doi.org/10.1371/journal.pone.0044207>.

Sharma, H.S., Sharma, A., 2012. Neurotoxicity of engineered nanoparticles from metals. *CNS Neurol. Disord. Drug Targets* 11, 65–80. <http://dx.doi.org/10.2174/187152712799960817>.

Shi, L.H., Perin, J.C., Leipzig, J., Zhang, Z., Sullivan, K.E., 2011. Genome-wide analysis of interferon regulatory factor 1 binding in primary human monocytes. *Gene* 487, 21–28. <http://dx.doi.org/10.1016/j.gene.2011.07.004>.

Skalska, J., Frontczak-Baniewicz, M., Struzynska, L., 2015. Synaptic degeneration in rat brain after prolonged oral exposure to silver nanoparticles. *Neurotoxicology* 46, 145–154. <http://dx.doi.org/10.1016/j.neuro.2014.11.002>.

Steinerman, J.R., Irizarry, M., Scarimeas, N., Raju, S., Brandt, J., Albert, M., Blacker, D., Hyman, B., Stern, Y., 2008. Distinct pools of beta-amyloid in Alzheimer disease-affected brain: a clinicopathologic study. *Arch. Neurol.* 65, 906–912. <http://dx.doi.org/10.1001/archneur.65.7.906>.

Tryndyk, V.P., Beland, F.A., Pogribny, I.P., 2010. E-cadherin transcriptional down-regulation by epigenetic and microRNA-200 family alterations is related to mesenchymal and drug-resistant phenotypes in human breast cancer cells. *Int. J. Cancer* 126, 2575–2583. <http://dx.doi.org/10.1002/ijc.24972>.

Vilaysane, A., Muruve, D.A., 2009. The innate immune response to DNA. *Semin. Immunol.* 21, 208–214. <http://dx.doi.org/10.1016/j.smim.2009.05.006>.

Wang, Y., Wang, B., Zhu, M.T., Li, M., Wang, H.J., Wang, M., Ouyang, H., Chai, Z.F., Feng, W.Y., Zhao, Y.L., 2011. Microglial activation, recruitment and phagocytosis as linked phenomena in ferric oxide nanoparticle exposure. *Toxicol. Lett.* 205, 26–37. <http://dx.doi.org/10.1016/j.toxlet.2011.05.001>.

Weiss, N., Miller, F., Cazaubon, S., Couraud, P.O., 2009. The blood–brain barrier in brain homeostasis and neurological diseases. *Biochim. Biophys. Acta* 1788, 842–857. <http://dx.doi.org/10.1016/j.bbamem.2008.10.022>.

Wilkins, H.M., Marquardt, K., Lash, L.H., Linseman, D.A., 2012. Bcl-2 is a novel interacting partner for the 2-oxoglutarate carrier and a key regulator of mitochondrial glutathione. *Free Radic. Biol. Med.* 52, 410–419. <http://dx.doi.org/10.1016/j.freeradbiomed.2011.10.495>.

Wiltfang, J., Esselmann, H., Bibl, M., Hull, M., Hampel, H., Kessler, H., Frolich, L., Schroder, J., Peters, O., Jessen, F., Luckhaus, C., Perneczky, R., Jahn, H., Fiszer, M., Maler, J.M., Zimmermann, R., Bruckmoser, R., Kornhuber, J., Lewczuk, P., 2007. Amyloid beta peptide ratio 42/40 but not A beta 42 correlates with phospho-Tau in patients with low- and high-CSF A beta 40 load. *J. Neurochem.* 101, 1053–1059. <http://dx.doi.org/10.1111/j.1471-4159.2006.04404.x>.

Wu, B., Yamaguchi, H., Lai, F.A., Shen, J., 2013. Presenilins regulate calcium homeostasis and presynaptic function via ryanodine receptors in hippocampal neurons. *Proc. Natl. Acad. Sci. U. S. A.* 110, 15091–15096. <http://dx.doi.org/10.1073/pnas.1304171110>.